Highly Crystalline Cubic Mesoporous TiO_2 with 10-nm Pore Diameter Made with a New Block Copolymer Template

Bernd Smarsly,*,† David Grosso,*,‡ Torsten Brezesinski,† Nicola Pinna,† Cédric Boissière,‡ Markus Antonietti,† and Clément Sanchez‡

Max Planck Institute of Colloids and Interfaces, Research Campus Golm, D-14424 Potsdam, Germany, and Laboratoire Chimie de la Matière Condensée, Université Pierre et Marie Curie, 4 place Jussieu, 75252 Paris Cedex 5, France

Received March 11, 2004. Revised Manuscript Received April 29, 2004

A strategy is shown to fabricate highly organized mesoporous anatase films exhibiting favorable properties for photocatalysis and photovoltaic applications by the hydrolysis/condensation of $TiCl_4$ in the presence of PHB−PEO block copolymer templates. Dipcoating for evaporation-induced-self-assembly followed by a straight thermal treatment was employed. The evaporation/structuration process and the thermal treatment were mechanistically followed by in situ GISAXS/WAXS measurements, and the final product was carefully analyzed by spectroscopic ellipsometry and transmission electron microscopy to reveal the consequences of crystallization onto the micro-, the meso-, and the macroscale.

Introduction

Increasing interest in the field of photovoltaic cells, photocatalysis, and gas sensors to supplant conventional methods has motivated the design of new devices involving nanostructured crystalline TiO_2 materials. The ideal material would be porous and highly crystalline and would present a high surface-to-volume ratio as to enhance exchange with a second phase or the environment. An optimal structure for photovoltaics would possess a pore and wall thickness of about 10 nm, which is the exciton diffusion length of titania. For instance, this strategy would allow the fabrication of structurally optimized photovoltaic cells, made from conjugated organic p-conductors infiltrated into mesoporous titania.[1] For both sensor and photovoltaic applications, the applied porous titania films should be homogeneous and should have a thickness between 100 nm and some micrometers. This can be provided by the so-called evaporation induced self-assembly (EISA) technique, which has already proven to be very efficient to prepare organized thin films of inorganic materials, using organic surfactant micelles as template.[2] Mesoporous anatase thin films and powders were prepared through this technique from $TiCl_4$ precursors and PEO−PPO surfactants[3] and other TiO_2 precursors.[4] The crystallization takes place at high temperature (450−550 °C) and is always accompanied by high shrinkage of the mesostructure and is eventually followed by its total collapsing at higher temperatures due to extensive growth of nanocrystals. The preparation of a highly pure and organized nanocrystalline porous network was shown to be possible up to now only by very careful control of the different steps of thermal treatment (optimal sequence involving certain time at specific temperatures). In such conditions, the initial three-dimensional initial template structure is transformed into a gridlike structure through an epitaxial pore fusion process, the maximal pore size obtained being around 7 nm with the largest commercially available PEO−PPO−PEO (F127) amphiphile.[3] However, the preparation of such materials requires several carefully chosen steps and is time-consuming. It is important to mention that the fabrication of crystalline mesoporous titania often fails because of the sensitivity of the structure toward the heat treatment procedure and crystallization.

The key problem throughout these syntheses is that titania has a rather low nucleation-to-growth rate, making bulk nanoparticles grow to a diameter of 10−20 nm. If such a process starts in much thinner titania walls of a mesoporous system, it is evident that the

* To whom correspondence should be addressed. E-mail, smarsly@mpikg-golm.mpg.de; tel., +49 331 567 9508; fax, +49 331 567 9502 (B. Smarsly). E-mail, grosso@ccr.jussieu.fr; tel., +33 (0) 1 44 27 55 42 (D. Grosso).

† Max Planck Institute of Colloids and Interfaces.

‡ Université Pierre et Marie Curie.

(1) Coakley, K. M.; McGehee, M. D. *Appl. Phys. Lett.* **2003**, *83*, 3380.

(2) Brinker, C. J.; Lu, Y. F.; Sellinger, A.; Fan, H. Y. *Adv. Mater.* **1999**, *11*, 579.

(3) (a) Grosso D.; Soler-Illia, G. J. D. A.; Crepaldi, E. L.; Cagnol, F.; Sinturel, C.; Bourgeois, A.; Brunet-Bruneau, A.; Amenitsch, H.; Albouy, P. A.; Sanchez, C. *Chem. Mater.* **2003**, *15*, 4562. (b) Crepaldi, E. L.; Soler-Illia, G. J. D. A.; Grosso, D.; Cagnol, F.; Ribot, F.; Sanchez, C. *J. Am. Chem. Soc.* **2003**, *125*, 9770. (c) Soler-Illia, G. J. D. A.; Crepaldi, E. L.; Grosso, D.; Sanchez, C. *Curr. Opin. Colloid Interface Sci.* **2003**, *8*, 109. (d) Crepaldi, E. L.; Soler-Illia, G. J. D. A.; Grosso, D. Sanchez, C. *New J. Chem.* **2003**, *27*, 9. (e) Grosso, D.; Babonneau, F.; Sanchez, C.; Soler-Illia, G. J. D. A.; Crepaldi, E. L.; Albouy, P. A.; Amenitsch, H.; Balkenende, A. R.; Brunet-Bruneau, A. *J. Sol−Gel. Sci. Technol.* **2003**, *26*, 561. (f) Crepaldi, E. L.; Soler-Illia, G. J. D. A.; Grosso, D.; Albouy, P. A.; Amenitsch, H.; Sanchez, C. *Stud. Surf. Sci. Catal.* **2002**, *141*. 235. (g) Sanchez, C.; Soler-Illia, G. J. D. A.; Ribot, F.; Grosso, D. *C. R. Acad. Sci. Chim.* 2003, 8, 109.

(4) (a) Alberius, P. C. A.; Frindell, K. L.; Hayward, R. C. E.; Kramer, J.; Stucky, G. D.; Chmelka, B. F. *Chem. Mater.* **2002**, *14*, 3284. (b) Coakley, K. M.; Liu, Y. X.; McGehee, M. D.; Frindell, K. L.; Stucky, G. D. *Adv. Funct. Mater.* **2003**, *13*, 301. (c) Bosc, F.; Ayral, A.; Albouy, P. A.; Guizard, C. *Chem. Mater.* **2003**, *15*, 2463.

10.1021/cm0495966 CCC: $27.50
Published on Web 07/01/2004

primary structure is lost throughout the crystallization process, partly due to the mass transport in the walls and partly due to the missing connectivity between the nanoparticles. There are two complementing solutions for this problem. Either the conditions of sol chemistry are changed in a way that the preformed "amorphous" titania structures are better interlinked and show a molecular preorganization which supports faster nucleation. This can be done by reducing the water content in the recipes, for instance, by addition of *tert*-butyl alcohol[5] or in ionic liquids.[6] The other possibility is the development of new templates promoting larger pore sizes which self-organize sufficiently early in the process to support a robust titania gel structure. Note that also the first solution would strongly benefit from more robust templates, as the addition of alcohols and organic solvents usually interferes with the template organization process.

In the present work we want to make a first step into this direction and employ a new block copolymer template for the preparation of mesoporous titania of sufficient size to allow free titania nucleation within the walls. We use novel PHB−PEO block copolymers (based on the commercial Kraton liquid block). These polymers were described to generate a highly ordered fcc lattice of spherical pores with a diameter of ca. 13−14 nm and tuneable wall thickness in silica.[7] In addition, the micelles of these block copolymers show better temperature stability and a lower alcohol sensitivity and also possess a higher hydrophobic contrast than Pluronic-type copolymers (the standard system), thus leading to a greater driving force for self-assembly. It will be shown that these block copolymers are highly suitable templates for the EISA process and allow the preparation of mesoporous anatase with high crystallinity and significantly larger pores than previously reported in a short and basic processing, thus adjusting the titania material to the natural exciton length scale as a result of the initial template dimension. Various analytical techniques are applied to study the structure formation and its temperature resistance, including TEM, HR-TEM, spectral ellipsometry, in situ WAXS, and grazing incidence SAXS (GISAXS).

Experimental Section

PHB−PEO block copolymers ($H(CH_2CH_2CH_2CH(CH_3)CH_3)_{66}(OCH_2CH_2)_{86}H$) (referred to also as "KLE") were prepared by coupling "Kraton Liquid" (*ω*-hydroxypoly(ethylene-*co*-butylene), Exxon) with ethylene oxide using an anionic polymerization procedure. Both blocks are narrowly distributed, with $M_w = 3700$ g/mol for the polyethylene-*co*-butylene block and $M_w = 3780$ g/mol for the polyethylenoxide block. For further details, see ref 7.

The mesoporous TiO_2 thin films were prepared by dipcoating at constant speed (2 mm·s^{-1}) and constant relative humidity (RH = 40%) from solutions typically composed in a molar ratio of 1:27:14:5:(6.6×10^{-3}) $TiCl_4$ (Fluka >98%):EtOH:THF:H_2O:B_{66}−EO_{86}. As-prepared and calcined films were then characterized by XRD (low and wide angles (Bruker D8)), 2D-SAXS (Elettra synchrotron facilities), and ellipsometry (Woollam-VASE M-2000U). A Philips CM200 FEG microscope, 200 kV, equipped with a field emission gun was used for HRTEM. Transmission electron microscopy (TEM) images with high contrast were taken with a Zeiss EM 912Ω at an acceleration voltage of 120 kV. Samples were ground in a ball-mill and taken up in acetone. One droplet of the suspension was applied to a 400-mesh carbon-coated copper grid and left to dry in air.

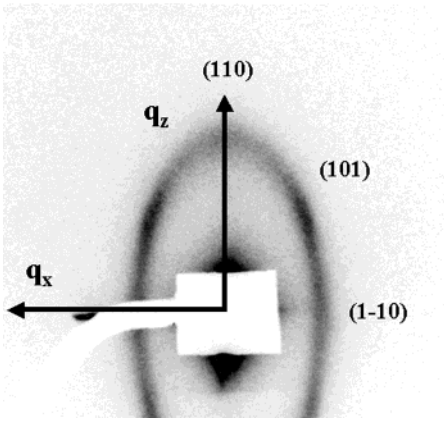

Figure 1. GISAXS 2D pattern of a film prepared at 40% RH and dried at 100 °C. The typical diffraction spots of a bcc *Im*3*m* structure are present with the corresponding circular permutation.

Results and Discussion

The mesostructures were studied by grazing-incidence small-angle X-ray scattering (GISAXS), using the Elettra synchrotron SAXS line (Trieste, Italy). The mesostructuration of the KLE templated TiO_2 thin films was followed by collecting diffraction patterns of the film at a 5° incident angle every 2 s during the evaporation process, following the experimental procedure described previously.[3] Briefly, this investigation requires the use of the high flux at 8 keV of the Elettra synchrotron's SAXS line, a specific dipcoater in which the relative humidity is controlled and ultrathin Si wafers (10-*μ*m thick) standing as fixed substrates while solutions are lowered underneath. This investigation (not shown here) revealed that a mesostructure is formed only when the relative humidity (RH) is maintained between 30 and 60%, confirming the crucial role of the water vapor pressure of the environment during EISA, already observed for silica[8] and titania systems.[3] A very interesting point concerns the rapidity with which the present KLE copolymer self-assembles and drives the hybrid system to meso-organize. Indeed, the process of mesostructuration starts close to the drying line, typically 30 s after coating, and needs only several seconds to be completed, while the same system, using Pluronic F127, starts to organize only after 2−3 min and is completed after an additional minute. This fast self-assembly of the present template is likely to be attributed to the enhanced hydrophobic character of the PHB chain.

Films prepared under these optimal conditions (see Experimental Section) present the characteristic XRD pattern of the bcc *Im*3*m* structure with a lattice parameter of $a = 285$ Å ($d(110) = 200$ Å) as shown in Figure 1. The diffraction spots correspond to domains

(5) Dag, O.; Soten, I.; Celik, O.; Polarz, S.; Coombs, N.; Ozin, G. A. *Adv. Funct. Mater.* **2003**, *13*, 30.
(6) Zhou, Y.; Antonietti, M. *J. Am. Chem. Soc.* **2003**, *49*, 14960.
(7) Thomas, A.; Schlaad, H.; Smarsly, B.; Antonietti, M. *Langmuir* **2003**, *19*, 4455.
(8) Cagnol, F.; Grosso, D.; Soler-Illia, G. J. D. A.; Crepaldi, E. L.; Babonneau, F.; Amenitsch, H.; Sanchez, C. *J. Mater. Chem.* **2003**, *13*, 61.

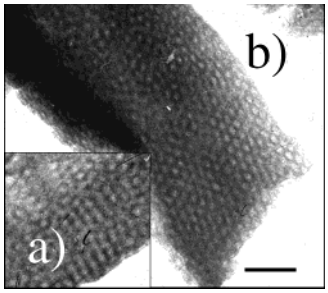

Figure 2. TEM images of a film treated at 100 °C, scratched off the surface, and deposited on a C-deposited copper TEM grid before analysis, revealing the [110] zone axis (a) and the [111] zone axis (b). The scale bar corresponds to 100 nm.

showing the [110] direction normal to the surface. The faint ellipsoidal circle corresponds to domains that have the same structure, but with random orientation with respect to the surface. These poly-oriented domains result from the fast organization described above, leading to a short time (a few seconds) for the organized domains to align themselves homogeneously with the air and substrate interfaces. The pattern is vertically contracted as a result of the drying forces of such a system. Because of that, the real structure is no more *Im*3*m* cubic and transforms into a face-centered orthorhombic.[3] Nevertheless, the *Im*3*m* indexing is used for simplicity.

The contracted cubic structure is confirmed by TEM analysis in Figure 2 where one can clearly observe the hexagonal array on the [111] zone axis and the corresponding cubic array on the [110] zone axis.

Crystallization. The removal of the copolymer template by calcination and the crystallization of the walls into nanocrystalline anatase require a thermal treatment at temperatures above 400 °C. As determined by thermogravimetric analysis, the polymer is completely decomposed at 400 °C in air. To assess the evolution of the mesostructure during crystallization, thin films were treated in a specially designed furnace within the Elettra SAXS beam line. A CCD camera collected in situ the small-angle diffraction patterns (mesostructure), while a linear detector was placed as to simultaneously record the wide-angle diffraction diagrams (crystalline microstructure). Thus, the presence of the mesostructure and the crystallization could be monitored in situ as a function of the temperature. The heating ramp was fixed at 8 °C min^{-1} (under air). The results are shown in Figure 3. More details on such an experiment can be found elsewhere.[3]

The WAXS data reveal that the crystallization into anatase takes place at 450 °C and that no other crystalline phases (brookite or rutile) are observed even at a temperature of 700 °C. This speaks for the very high stability of anatase within the scaffold. Because of the low resolution in fwhm, which depends on the beam size, the sample dimension, and the grazing angle, no estimate of the crystal size according to the Scherrer formulas can be given.

Concerning the mesostructure, one observes first a high unidirectional shrinkage normal to the surface. This contraction is quasi-linear with the temperature and reaches 40% at 450 °C and 60% above 600 °C. This is well above the minimal shrinkage, which is related to the cross-linking and rearrangement of oxo-titanate species (the density difference between crystalline anatase of ca. 3.7 g/mL and amorphous titania), and

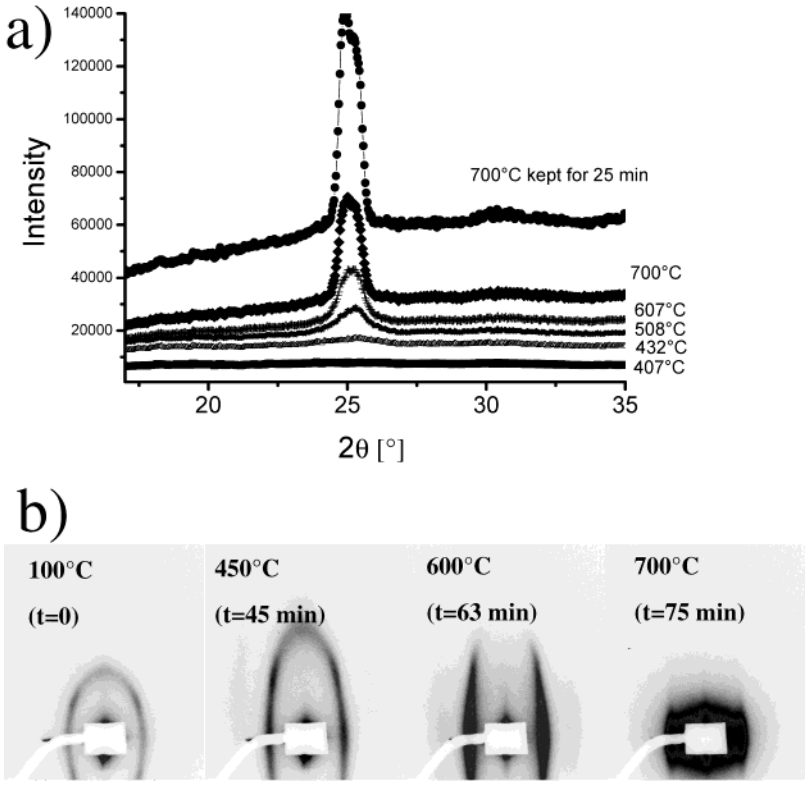

Figure 3. In situ WAXS (101 reflection, a) and 2D GISAXS (b) investigation performed during thermal treatment of the *Im*3*m* cubic TiO_2 films as a function of the thermal treatment. The film was heat-treated up to 700 °C after drying overnight at 100 °C ($t = 0$). The orientation of the film is equivalent to Figure 1. In Figure 3a, it is seen that keeping the film at 700 °C for a longer time (25 min) leads to an increase in the crystallinity.

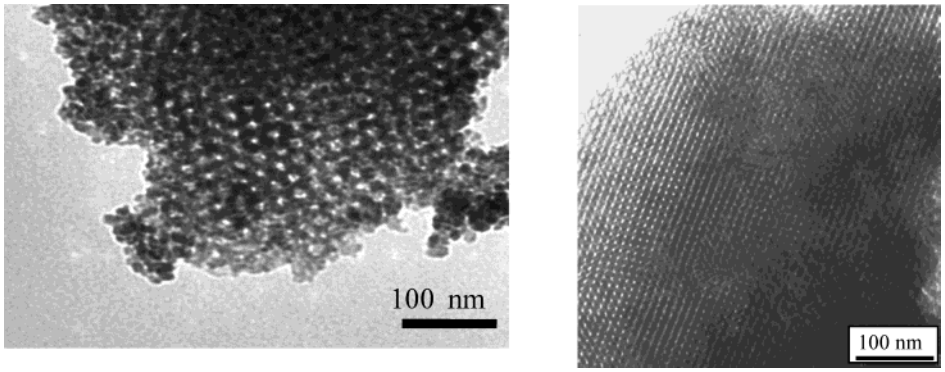

Figure 4. TEM analysis of the 450 °C calcined sample showing the contracted *Im*3*m* structure.

corresponds to mass transport due to crystallization. Here, further improvement will just be possible by improving the chemical sol−gel recipes, which is however out of the scope of the present contribution.

Despite this contraction that promotes the transformation from cubic to orthorhombic, it was observed that the diffraction spots are still well-defined at 450 °C (temperature of crystallization). The epitaxial pore fusion observed for the anatase/Pluronic F127 system,[3] which was attributed to the diffuse sintering following the crystallization step, can also be found in the present KLE-TiO_2 system, but occurs at higher temperatures. The transformation, identified by the merging of the in-plane (101) diffraction spot and the off-plane ($1\bar{1}0$) diffraction spots, starts to occur at 600 °C and is completed at 700 °C; only the ($1\bar{1}0$) diffraction spots are left, as depicted in Figure 3. Higher temperatures or an extended residence time at 700 °C leads to the collapse of the whole mesostructure through extensive microcrystalline particle growth.

To allow crystallization with a minimum of mesostructure transformation, a sample was dried at 100 °C overnight and thermally treated at 450 °C for 2 h under air. The corresponding 2D GISAXS pattern is similar to the one shown in Figure 3 (450 °C), except for the observation that the contraction of the network was 60%. On the other hand, the diffraction spots are still well-defined, suggesting that no pore merging took place.

These results are corroborated by the TEM and HRTEM investigations in Figures 4 and 5. It is nicely seen that the contracted *Im*3*m* structure is retained after the template removal. Figure 4 shows a representative part of the mesostructure. As compared to the noncrystallized counterpart, the walls seem to be thicker, composed of nonregular crystals. This goes well with a structural densification by a factor of 2. Selected area electron diffraction (Figure 5b) displays diffraction rings characteristic of a structure composed of little domains with the crystallographic axis randomly oriented with respect to each other. The *d* spacings determined from the diffraction rings are in good agreement with the anatase structure. HRTEM of a single nanodomain (Figure 5c) shows sets of lattice fringes, giving additional evidence that the domains are highly crystallized. The power spectrum (Figure 5d) of such domain shows several reflections characteristic of the anatase structure oriented along the [100] direction; it reveals that the domain is monocrystalline and in perfect mutual contact with each other. From all the TEM it is

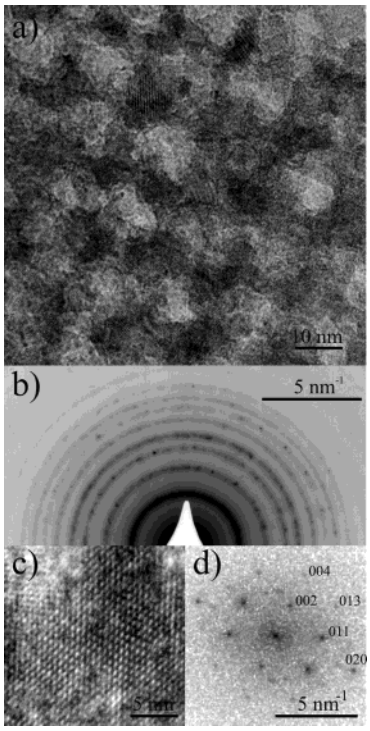

Figure 5. HRTEM pattern of a representative part of the mesostructure (a), selected area electron diffraction of a zone of 250 nm of diameter (b), HRTEM image of a single domain (c), and its power spectrum (d).

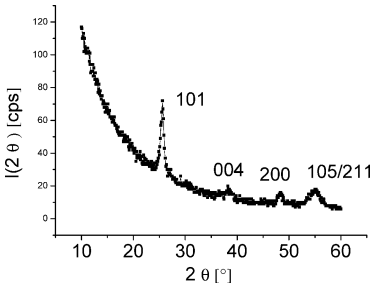

Figure 6. XRD diagram of film calcined 2 h at 450 °C taken in Bragg Brentano geometry using Sollar slits and the incident beam irradiation being fixed at 0.3°.

concluded that the entire matrix between the mesopores is composed of anatase crystalline nanodomains of about 5−10 nm in size. This corresponds well with the domain size (ca. 10 nm) obtained from XRD by applying the Scherrer equation.

Figure 6 shows a wide-angle X-ray scattering pattern of the calcined film, suggesting that no amorphous

inorganic species are left. Thus, HRTEM and XRD indicate the presence of a well-defined mesopore network with a crystalline matrix between the mesopores. Although the data do not allow a precise quantification of the crystallinity, the content in amorphous TiO_2 was estimated to be on the order of only several percent in volume fraction at the most, based on a comparison of Figure 6 with the XRD of amorphous TiO_2 (not shown). Further X-ray studies are dedicated to an exact determination of the crystallinity.

Ellipsometry investigations revealed that the initial thickness of 200 nm was reduced to about 90 nm after thermal treatment (2 h at 450 °C), suggesting a contraction of 55% normal to the substrate surface. Therefore, macroscopic and mesoscopic shrinkage agree well. From the ellipsometric measurements, also the overall porosity was estimated, using the Bruggeman effective medium approximation and combining the optical constants of anatase and those of voids. A value of 35 vol % was calculated after the thermal treatment.

The band gap of the mesostructured anatase TiO_2 was determined by ellipsometry. Since anatase TiO_2 is an indirect band gap semiconductor, the value $(\alpha h\nu)^{1/2}$ is plotted versus $h\nu$, where α is the absorption coefficient and $h\nu$ the photon energy (deduced from the dispersion plot of the extinction coefficient by ellispometry analysis). The extrapolation of the decreasing slope to zero gives the E_g value; we obtained a band gap of 3.4 eV.

Conclusions

A strategy is presented which allows the preparation of porous TiO_2 thin films with a well-defined contracted *Im*3*m* mesostructure and a crystalline anatase framework between the mesopores. The mesopore size is about 10 nm determined from TEM and thereby larger than that in previously reported crystalline TiO_2 materials with an ordered mesostructure.[9,10] The determination of the exact pore size and the accessible porosity will be subject to closer investigation in a separate study. Also, the mesostructure turned out to be stable up to 700 °C. Not only did the employed KLE block copolymer result in significantly larger mesopores but also its self-assembly was fast and rather resistant against the solvent in the recipe. This is attributed to the enhanced hydrophobic attraction between the hydrophobic polymer chains, as compared to Pluronics. An indirect measure for this stability is that complete crystallization upon template revomal of TiO_2 and the stability of the final porous mesostructure was achieved by a simple heat-treatment procedure, while in previous studies a complex temperature program was necessary to avoid a mesostructure collapse.

The remaining shrinkage was quantified and is believed to be improved by changes in the sol−gel recipe, only, such as starting from preorganized titania cluster (the nanobuilding block approach)[11,12] or adding specific alcohols/solvents to change hydration and condensation motifs, which is possible with the present robust template. Forthcoming work addresses these details of the role of various chemical parameters (external humidity, alcohol content, type of alcohol, etc.) on the interplay of mesostructure formation and inorganic polyreaction to improve shrinking behavior and mechanical stability of functional crystalline mesoporous inorganics.

Supporting Information Available: Figures of mesoporous TiO_2 with crystalline walls (PDF). This material is available free of charge via the Internet at http://pubs.acs.org.

CM0495966

(9) Yu, C. Z.; Tian, B. Z.; Zhao, D. Y. *Curr. Opin. Solid State Mater. Sci.* **2003**, *7*, 191.
(10) Yang, P. D.; Deng, T.; Zhao, D. Y.; Feng, P. Y.; Pine, D.; Chmelka, B. F.; Whitesides, G. M.; Stucky, G. D. *Science* **1998**, *282*, 2244.
(11) Sanchez, C.; Soler-Illia, G. J. A. A.; Ribot, F.; Lalot, T.; Mayer, C. R.; Cabuil, V. *Chem. Mater.* **2001**, *13*, 3061.
(12) Steunou, N.; Förster, S.; Florian, P.; Sanchez, C.; Antonietti., M. *J. Mater. Chem.* **2002**, *12*, 3426.